

# Efficiency of the CO<sub>2</sub>-concentrating mechanism of diatoms

Brian M. Hopkinson<sup>a,1</sup>, Christopher L. Dupont<sup>b</sup>, Andrew E. Allen<sup>b</sup>, and François M. M. Morel<sup>a,2</sup>

<sup>a</sup>Department of Geosciences, Princeton University, Princeton, NJ 08544; and <sup>b</sup>J. Craig Venter Institute, San Diego, CA 92121

This contribution is part of the special series of Inaugural Articles by members of the National Academy of Sciences elected in 2009.

Contributed by François M. Morel, January 19, 2011 (sent for review October 1, 2010)

**Diatoms are responsible for a large fraction of CO<sub>2</sub> export to deep seawater, a process responsible for low modern-day CO<sub>2</sub> concentrations in surface seawater and the atmosphere. Like other photosynthetic organisms, diatoms have adapted to these low ambient concentrations by operating a CO<sub>2</sub> concentrating mechanism (CCM) to elevate the concentration of CO<sub>2</sub> at the site of fixation. We used mass spectrometric measurements of passive and active cellular carbon fluxes and model simulations of these fluxes to better understand the stoichiometric and energetic efficiency and the physiological architecture of the diatom CCM. The membranes of diatoms are highly permeable to CO<sub>2</sub>, resulting in a large diffusive exchange of CO<sub>2</sub> between the cell and external milieu. An active transport of carbon from the cytoplasm into the chloroplast is the main driver of the diatom CCM. Only one-third of this carbon flux is fixed photosynthetically, and the rest is lost by CO<sub>2</sub> diffusion back to the cytoplasm. Both the passive influx of CO<sub>2</sub> from the external medium and the recycling of the CO<sub>2</sub> leaking out of the chloroplast are achieved by the activity of a carbonic anhydrase enzyme combined with the maintenance of a low concentration of HCO<sub>3</sub><sup>-</sup> in the cytoplasm. To achieve the CO<sub>2</sub> concentration necessary to saturate carbon fixation, the CO<sub>2</sub> is most likely concentrated within the pyrenoid, an organelle within the chloroplast where the CO<sub>2</sub>-fixing enzyme is located.**

climate change | ocean acidification | phytoplankton

**D**iatoms evolved during the Mesozoic era and have gradually become major actors in the oceanic cycles of elements (1). Their precipitation of siliceous frustules now dominates the reverse weathering of silica, and their photosynthetic activity contributes some 40% of modern-day oceanic primary production. Because of their large size and silica ballast, they contribute a major fraction of the downward flux of particulate organic carbon and thus, a major fraction of the export of CO<sub>2</sub> to deep seawater. The low modern-day CO<sub>2</sub> concentration in surface seawater and the atmosphere that results from this biological carbon pump poses a challenge to photosynthetic organisms, including diatoms themselves. Like most photosynthetic organisms, they fix carbon using RubisCO as the carboxylating enzyme. Diatom RubisCOs suffer from the same slow turnover rate and wasteful tendency to fix O<sub>2</sub> as other RubisCOs, and their affinity for CO<sub>2</sub> is only marginally better (2, 3). As in other photosynthetic organisms, the main adaptation of diatoms to the gradual decrease in ambient CO<sub>2</sub> and increase in O<sub>2</sub> over geological times has been the evolution of a CO<sub>2</sub> concentrating mechanism (CCM) to elevate the concentration of CO<sub>2</sub> at the site of fixation by RubisCO (4–7). It is perhaps not an exaggeration to posit that today's atmospheric CO<sub>2</sub> concentration is, in large part, determined by the efficiency of the CCM of diatoms.

Despite its importance, the physiology/biochemistry of diatoms has been little studied compared with that of model photosynthetic organisms, and the CCM of diatoms is still poorly understood. Some species operate a C<sub>4</sub>-type pathway, whereas others seem to rely on active transport of HCO<sub>3</sub><sup>-</sup> into the chloroplast (4–8). Active transport of inorganic carbon by the CCM is thought to account for a significant portion of cellular energy expenditure (2). Energy expenditure on the CCM is

currently of interest, because savings from its down-regulation are likely to be responsible for the major acclimations of oceanic phytoplankton to rising CO<sub>2</sub> over the next century.

Because lipid bilayers are highly permeable to small uncharged molecules like CO<sub>2</sub> (9), the CCM of unicellular organisms like diatoms is necessarily leaky; only a fraction of the CO<sub>2</sub> molecules concentrated at the site of RubisCO end up being fixed, and the rest are lost by diffusion. The total energetic expenditure to operate a CCM is, thus, the product of the energy expended to concentrate 1 molecule CO<sub>2</sub> at the site of fixation multiplied by the mole ratio of CO<sub>2</sub> transported to CO<sub>2</sub> fixed. However, at this point, neither of these terms is known with any precision. At the most basic level, we do not know how permeable to CO<sub>2</sub> diatoms membranes really are and what barriers may slow down the outward diffusion of CO<sub>2</sub> (10, 11). Here, we attempt a complete characterization of inorganic carbon fluxes in model diatoms using membrane inlet MS (MIMS) (12) and kinetic models of <sup>18</sup>O isotope exchange from CO<sub>2</sub>.

## Results

**Overall Strategy.** The bulk of our experiments consist of time courses of <sup>18</sup>O depletion from labeled inorganic carbon, a process catalyzed by the presence of the enzyme carbonic anhydrase (CA) in cells. CA, which catalyzes the hydration of CO<sub>2</sub> and dehydration of HCO<sub>3</sub><sup>-</sup>, plays critical roles in CCMs and is present in all our experimental organisms: *Thalassiosira weissflogii*, *T. pseudonana*, *T. oceanica*, and *Phaedacylum tricornutum*, (*SI Text, Experimental Organisms*). The <sup>18</sup>O depletion data are analyzed quantitatively using either a one- (homogenous intracellular compartment) or two-compartment (cytoplasm and chloroplast) model depending on the data. In a first set of experiments with suspensions of cells in the dark (i.e., no photosynthesis), we determine the permeability of the cytoplasmic membranes to CO<sub>2</sub> and HCO<sub>3</sub><sup>-</sup>. Additional dark experiments with a strain of *P. tricornutum* overexpressing a chloroplast-localized CA provide constraints on the permeability of the chloroplast envelope. A third set of experiments with *P. tricornutum* suspensions in the light is used to determine active fluxes of inorganic carbon into the cytoplasm and chloroplast.

**Dark Experiments: Permeability of the Cytoplasmic Membrane.** On introduction of dissolved inorganic carbon (DIC) labeled with <sup>13</sup>C and <sup>18</sup>O into unlabeled water buffered at pH 8.0, the labeled species, CO<sub>2</sub>, HCO<sub>3</sub><sup>-</sup>, and CO<sub>3</sub><sup>2-</sup>, reach chemical and isotopic equilibrium with each other within minutes. Over a time scale of hours (Fig. 1A, left side), <sup>18</sup>O is lost from DIC as a result of the incorporation of <sup>16</sup>O during the hydration of CO<sub>2</sub> by H<sub>2</sub><sup>16</sup>O and

Author contributions: B.M.H. and F.M.M.M. designed research; B.M.H., C.L.D., and A.E.A. performed research; B.M.H. and F.M.M.M. analyzed data; and B.M.H. and F.M.M.M. wrote the paper.

The authors declare no conflict of interest.

<sup>1</sup>Present address: Department of Marine Sciences, University of Georgia, Athens, GA 30602.

<sup>2</sup>To whom correspondence should be addressed. E-mail: morel@princeton.edu.

This article contains supporting information online at [www.pnas.org/lookup/suppl/doi:10.1073/pnas.1018062108/-DCSupplemental](http://www.pnas.org/lookup/suppl/doi:10.1073/pnas.1018062108/-DCSupplemental).

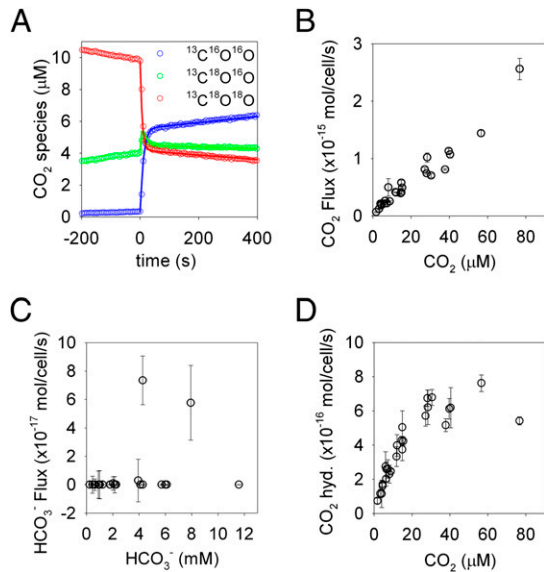


**Fig. 1.** Results of dark experiments to determine passive inorganic carbon fluxes. (A) A sample fit (solid lines) of a single-compartment model, described in *SI Text, One-Compartment Models, Passive Carbon Fluxes* and diagrammed in Fig. 2, to  $^{18}\text{O}$ - $\text{CO}_2$  data (cells added at  $t = 0$ ). Inorganic carbon fluxes, derived from the model, as a function of extracellular carbon concentrations: (B)  $\text{CO}_2$  flux across the cytoplasmic membrane, (C)  $\text{HCO}_3^-$  flux across the cytoplasmic membrane, and (D) intracellular CA-catalyzed  $\text{CO}_2$  hydration rates. Error bars are the SE of the estimated fluxes.

subsequent dehydration of  $\text{HCO}_3^-$  ( $\text{HCO}_3^-$  and  $\text{CO}_3^{2-}$ , which equilibrate rapidly with each other, are treated as a combined pool, referred to as  $\text{HCO}_3^-$ ). Using MIMS, the time evolution of  $\text{CO}_2$  species with masses 49, 47, and 45 ( $^{13}\text{C}^{18}\text{O}^{18}\text{O}$ ,  $^{13}\text{C}^{18}\text{O}^{16}\text{O}$ , and  $^{13}\text{C}^{16}\text{O}^{16}\text{O}$ , respectively) provides a convenient means to study the kinetics of the hydration/dehydration of  $\text{CO}_2$  in the presence or absence of the enzyme CA, which catalyses the reaction (13, 14). If the experiment is carried out in the presence of cells that contain intracellular CA, the rate of  $^{18}\text{O}$  loss from  $\text{CO}_2$  provides information on both the kinetics of  $\text{CO}_2/\text{HCO}_3^-$  interconversion within the cell and the rate of passage of DIC species across the cellular membrane (13). As seen on the right side in Fig. 14, over the first 30 s after diatoms have been added to the assay medium (which contains the nonpenetrating inhibitor acetazolamide to inactivate external CA in addition to buffer and labeled DIC), there is a sudden depletion of  $^{18}\text{O}$  from the external  $\text{CO}_2$ . This decrease in  $^{49}\text{CO}_2$  in the medium is caused by rapid penetration of  $\text{CO}_2$  into the cells where it becomes depleted of  $^{18}\text{O}$  through hydration/dehydration cycles catalyzed by internal CA before diffusing out of the cells. This initial rapid phase terminates when the various isotopic species of  $\text{CO}_2$ , which diffuse rapidly across the external membrane, are equilibrated between the intracellular and external media. Subsequently, there is a further gradual depletion of  $^{18}\text{O}$  from  $\text{CO}_2$  resulting from a loss of  $^{18}\text{O}$  from extracellular  $\text{HCO}_3^-$ , which acts to buffer the  $^{18}\text{O}$  content of  $\text{CO}_2$  against depletion by CA, because the  $\text{HCO}_3^-$  concentration is  $>100\times$  that of  $\text{CO}_2$  at pH 8.0. The loss of  $^{18}\text{O}$  from  $\text{HCO}_3^-$  results from the background uncatalyzed hydration/dehydration of DIC in the external medium, the diffusion of  $^{18}\text{O}$ -depleted  $\text{CO}_2$  out of the cell, and the passage of  $\text{HCO}_3^-$  into the cell.

A quantitative analysis of the type of experimental data illustrated in Fig. 14 makes it possible to calculate the cellular transfer coefficients  $f_c$  and  $f_b$  ( $\text{cm}^2 \text{s}^{-1}$ ) of  $\text{CO}_2$  and  $\text{HCO}_3^-$  across the external membrane of the cells and the first-order rate constants  $k_{cf}$  and  $k_{cr}$  ( $\text{s}^{-1}$ ) for the CA-catalyzed rates of hydration and dehydration of  $\text{CO}_2/\text{HCO}_3^-$  inside the cells (Fig. 2 and Tables 1 and 2) (13). In the one-compartment model used for the analysis, CA

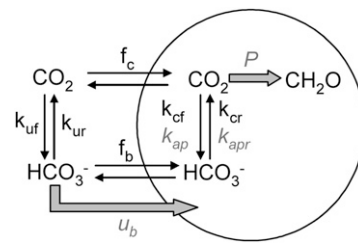


**Fig. 2.** Diagram of one-compartment models used to determine passive carbon fluxes and calculate  $k_{ap}$  during photosynthesis. Additional fluxes considered during photosynthesis are in gray and italicized.

is considered to be homogeneously distributed throughout the cell. The system of differential equations describing the behavior of  $^{18}\text{O}$ -DIC in the presence of CA-containing cells is presented in *SI Text, One-Compartment Models, Passive Carbon Fluxes* and Table S1 using the method by Tu et al. (13). This system is solved numerically by introducing in the equations appropriate geometric parameters for the cells (*SI Text, Experimental Organisms*). The calculated transfer coefficient  $f_c$  of  $\text{CO}_2$  across the cellular membrane is sufficiently large that diffusion of  $\text{CO}_2$  through the cell's boundary layer must be taken into account to calculate the permeability of the membrane to  $\text{CO}_2$ . This is done by considering that the observed  $f_c$  results from two transfer processes in series ( $1/f_c = 1/f_{c-BL} + 1/f_{c-M}$ ) and calculating the cellular transfer coefficient across the boundary layer from the diffusion coefficient of  $\text{CO}_2$ ,  $D$ , and the cell's equivalent radius,  $r$ :  $f_{c-BL} = 4\pi Dr$ . The membrane permeability to  $\text{CO}_2$ ,  $P_c$  (in  $\text{cm s}^{-1}$ ), is then obtained as the ratio of the cellular transfer coefficient across the membrane and the surface area of the cell:  $P_c = f_{c-M}/A$ .

According to our experimental data, the cytoplasmic membrane of diatoms is highly permeable to  $\text{CO}_2$ . Calculated values of  $P_c$  range between  $1.5 \times 10^{-2}$  and  $5.6 \times 10^{-2}$   $\text{cm/s}$  for the four species that we studied, indicating permeabilities that are just below those of artificial lipid membranes ( $\sim 10^{-1}$   $\text{cm/s}$ ) (9). These calculated  $P_c$  values may actually be underestimates if CA is not homogeneously distributed within the cell as assumed. For example, CA activity may be higher in the chloroplast, in which case the effective radius for diffusion through the boundary layer and the coefficient  $f_{c-BL}$  would be smaller. Regardless, it is clear that the cytoplasmic membrane does not present a significant barrier to  $\text{CO}_2$ . As a result, a DIC uptake system that would use a transmembrane  $\text{CO}_2$  transporter would be highly inefficient—akin to pouring water into a bottomless bucket.

In contrast, observed cellular transfer coefficients for passive transport of bicarbonate,  $f_b$ , are generally not significantly different from zero. As expected for a charged molecule,  $\text{HCO}_3^-$  does not pass easily through diatom membranes. The membranes of green algae are also effectively impermeable to  $\text{HCO}_3^-$  (10, 11). The upper limits of the measured  $f_b$  in our diatom species are several orders of magnitude lower than  $f_c$  values, such that the passive cellular fluxes of  $\text{HCO}_3^-$  can generally be neglected, although the concentration of  $\text{HCO}_3^-$  at pH 8 in seawater is  $140\times$  higher than  $\text{CO}_2$ . When passive  $\text{HCO}_3^-$  fluxes are neglected, the simplified system of equations describing  $\text{CO}_2$  fluxes across the membrane and intracellular CA activity can be solved analytically (*SI Text, One-Compartment Models, Analytical Approximation of Passive Fluxes*, Fig S1, and Table S2).

In the above analysis, DIC fluxes in and out of cells in the dark are assumed to be passive. This assumption can be tested by examining how cellular DIC fluxes vary with substrate concentration. In *P. tricornutum*, the  $\text{CO}_2$  influx is directly proportional to the extracellular  $\text{CO}_2$  concentration up to very high values (Fig. 1B), as expected for a passive flux, whether controlled by membrane permeability or diffusion in the boundary layer. In contrast, the  $\text{CO}_2$  flux should saturate at high concentration if it depended on active transport. The  $\text{HCO}_3^-$  influx is generally not significantly different from zero (Fig. 1C) and shows no trend with

**Table 1. Passive CO<sub>2</sub> fluxes in four diatoms**

Diatom	$f_c$ (cm <sup>3</sup> /s)	$f_{c-BL}$ (cm <sup>3</sup> /s)	$f_{c-M}$ (cm <sup>3</sup> /s)	$P_c$ (cm/s)
<i>P. tricornutum</i>	$2.3 \pm 0.4 \times 10^{-8}$	$7.7 \times 10^{-8}$	$3.3 \pm 0.4 \times 10^{-8}$	$3.1 \pm 0.4 \times 10^{-2}$
<i>T. weissflogii</i>	$6.3 \pm 3.2 \times 10^{-8}$	$1.5 \times 10^{-7}$	$1.1 \pm 0.3 \times 10^{-7}$	$2.4 \pm 0.7 \times 10^{-2}$
<i>T. pseudonana</i>	$1.8 \pm 0.6 \times 10^{-8}$	$5.0 \times 10^{-8}$	$2.8 \pm 0.6 \times 10^{-8}$	$5.6 \pm 1.1 \times 10^{-2}$
<i>T. oceanica</i>	$1.4 \pm 0.2 \times 10^{-8}$	$7.5 \times 10^{-8}$	$1.7 \pm 0.2 \times 10^{-8}$	$1.5 \pm 0.2 \times 10^{-2}$

The CO<sub>2</sub> influx, described by the cellular transfer coefficient  $f_c$  ( $\pm$  SD), is limited by diffusion through the boundary layer ( $f_{c-BL}$ ) and passage through the membrane ( $f_{c-M}$ ). The cytoplasmic membrane permeability to CO<sub>2</sub> ( $P_c \pm$  SD) is derived from  $f_{c-M}$ . At least four replicate measurements were made on each organism. Errors were propagated based on the error in  $f_c$  measurements.

HCO<sub>3</sub><sup>-</sup> concentration, suggesting that the occasional significant measurements are spurious. Such measurements may reflect incomplete inhibition of external CAs or damage to cell membranes during handling rather than true membrane permeability.

**Dark Experiments with Overexpressed Chloroplastic CA: Constraint on Chloroplast Membrane Permeability.** Because the subcellular location of CAs in diatoms is not generally known, the previous analyses considered the cell as a single compartment to compute the minimum permeability of the cytoplasmic membrane. To refine these results and estimate the permeability of the chloroplast envelope to CO<sub>2</sub>, we compared <sup>18</sup>O exchange assays in a *P. tricornutum* line overexpressing PtCA1, which is a chloroplastic  $\beta$ -CA (15), and the WT (Fig. 3). Greater CA activity was clearly detected in the PtCA1 overexpresser, indicating that the labeled DIC has access to the overexpressed CA. The system of equations describing <sup>18</sup>O exchange in a model with two cellular compartments (cytoplasm and chloroplast) and passive fluxes of both CO<sub>2</sub> and HCO<sub>3</sub><sup>-</sup> is underdetermined. Based on the results of the previous experiments, a simplified model in which only CO<sub>2</sub> fluxes across membranes are considered was used to interpret the data (Fig. 3B, Fig. S2, and SI Text, Chloroplast Envelope Permeability). This assumes that the chloroplast envelope, like the diatom cytoplasmic membrane, is impermeable to HCO<sub>3</sub><sup>-</sup>. Only a small passive HCO<sub>3</sub><sup>-</sup> flux across the chloroplast envelope is possible, because a large passive flux of a charged molecule would break down the necessary electrical gradient between the chloroplast and cytoplasm. In this simplified model, there are three unknowns ( $F_p$ , the flux of CO<sub>2</sub> into the chloroplast,  $F_{xi}$ , the CA-catalyzed rate of CO<sub>2</sub> hydration in the cytoplasm, and  $F_{xp}$ , the CA-catalyzed rate of CO<sub>2</sub> hydration in the chloroplast) and two equations relating the model parameters to <sup>18</sup>O-CO<sub>2</sub> observations (SI Text, Chloroplast Envelope Permeability). Because the assays with the WT and overexpresser were carried out at the same CO<sub>2</sub> concentrations, the rates of CO<sub>2</sub> hydration in the cytoplasm,  $F_{xi}$ , must also be the same, although the value is unknown. A possible range of values for  $F_p$  (and  $F_{xp}$ ) can then be obtained by varying  $F_{xi}$  between zero and the CO<sub>2</sub> hydration rate measured in the WT and minimizing error with <sup>18</sup>O-CO<sub>2</sub> observations. Alternatively, a minimum value for  $F_p$  is obtained if  $F_{xi}$  is taken to be the total CA activity in the WT and  $F_{xp} = \infty$ .

The range of calculated flux of CO<sub>2</sub> across the chloroplast membrane ( $0.4 \times 10^{-16}$  –  $2.1 \times 10^{-16}$  mol/cell per s) is between 10% and 50% of the maximal rate allowed by diffusion, implying

that this membrane is highly permeable to CO<sub>2</sub> (SI Text, Chloroplast Envelope Permeability). Like the cytoplasmic membrane, the chloroplast membrane has properties similar to artificial lipid bilayers and does not present a significant barrier to CO<sub>2</sub> diffusion. In what follows, we use a CO<sub>2</sub> transfer coefficient for the chloroplast implied by the lower limit of  $F_p$  ( $f_c = 6 \times 10^{-9}$  cm<sup>3</sup>/s) to see if, by itself, the diffusion barrier created by the chloroplast membrane could result in a sufficiently high concentration of CO<sub>2</sub> at the site of fixation (Discussion).

If the overexpressed CA was localized solely to the pyrenoid, our measurements could be used to constrain diffusive efflux of CO<sub>2</sub> from this compartment. Such localization is implied by the observation of the overexpressed protein, which was linked to CFP, as strongly fluorescent clusters inside the chloroplast stroma (15). The localization of PtCA1 to the pyrenoid was recently verified with immunogold labeling. Unfortunately, some fluorescence could also be detected outside the clusters, making it impossible to use the rate of CA-catalyzed <sup>18</sup>O loss to calculate CO<sub>2</sub> diffusion from the putative organelles.

**Experiments in the Light: Increase in CA Activity and Active Transport of DIC.** When light is turned on in a diatom suspension, one observes a transition phase of 30–60 s before steady state photosynthesis is reached (Fig. 4). During the transition phase, there is a rapid depletion of <sup>18</sup>O from CO<sub>2</sub> but little net O<sub>2</sub> production and no change in the total CO<sub>2</sub> concentration, indicating no significant net CO<sub>2</sub> flux into or out of the cells. The CCM and thylakoid pH gradient are presumably initiated during this time period, leading to <sup>18</sup>O depletion (Discussion). Later, during steady state photosynthesis, O<sub>2</sub> is produced at a constant rate, and total CO<sub>2</sub> is correspondingly drawn down. Because carbon is fixed from a CO<sub>2</sub> pool depleted of <sup>18</sup>O through exposure to CAs, <sup>13</sup>C<sup>16</sup>O<sup>16</sup>O accounts for the bulk of the drawdown. The observed <sup>18</sup>O depletion seen when light is turned on is commonly called light-stimulated CA activity (3, 7). This high apparent CA activity in the light can be caused either by an actual increase in intracellular CO<sub>2</sub> hydration/HCO<sub>3</sub><sup>-</sup> dehydration rates (i.e., CA activity) or active transport of DIC into a compartment with high CA activity. Extensive analysis of experimental data shows that both processes must be at play, and we examine them sequentially.

**Increase in CA Activity.** An increase in the activity of the cellular CA enzymes can plausibly be induced by light as a result of activation of CA or changes in the chemistry of cellular compart-

**Table 2. Passive HCO<sub>3</sub><sup>-</sup> fluxes in four diatoms**

Diatom	$f_b$ (cm <sup>3</sup> /s)	$f_{b-BL}$ (cm <sup>3</sup> /s)	$f_{b-M}$ (cm <sup>3</sup> /s)	$P_b$ (cm/s)
<i>P. tricornutum</i>	$0.4 \pm 1.1 \times 10^{-11}$	$4.6 \times 10^{-8}$	$0.4 \pm 1.1 \times 10^{-11}$	$0.4 \pm 1.0 \times 10^{-5}$
<i>T. weissflogii</i>	$1.3 \pm 1.2 \times 10^{-10}$	$8.9 \times 10^{-8}$	$1.3 \pm 1.2 \times 10^{-10}$	$2.9 \pm 2.7 \times 10^{-5}$
<i>T. pseudonana</i>	$1.3 \pm 2.0 \times 10^{-12}$	$3.0 \times 10^{-8}$	$1.3 \pm 2.0 \times 10^{-12}$	$2.5 \pm 3.9 \times 10^{-6}$
<i>T. oceanica</i>	$0.7 \pm 1.7 \times 10^{-11}$	$4.4 \times 10^{-8}$	$0.7 \pm 1.7 \times 10^{-11}$	$0.6 \pm 1.5 \times 10^{-5}$

The HCO<sub>3</sub><sup>-</sup> influx, described by the cellular transfer coefficient  $f_b$  ( $\pm$  SD), is limited by diffusion through the boundary layer ( $f_{b-BL}$ ) and passage through the membrane ( $f_{b-M}$ ). The cytoplasmic membrane permeability to HCO<sub>3</sub><sup>-</sup> ( $P_b \pm$  SD) is derived from  $f_{b-M}$ . At least four replicate measurements were made on each organism. Errors were propagated based on the error in  $f_b$  measurements.

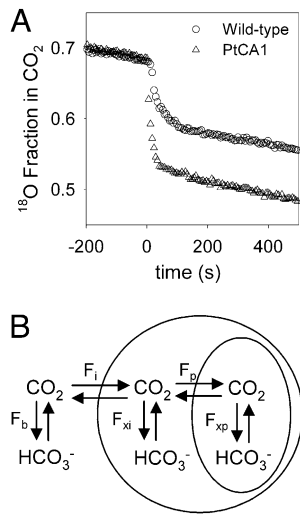


**Fig. 3.**  $^{18}\text{O}$  exchange in a *P. tricornutum* strain overexpressing PtCA1, a chloroplast localized CA. (A) A comparison of  $^{18}\text{O}$  depletion by WT and PtCA1 overexpressing *P. tricornutum*, and (B) a diagram of the model used to interpret the data. The assay was started by adding the same concentration of WT or PtCA1 overexpressing cells at  $t = 0$ .

ments, particularly changes in pH. To quantify the extent of such increase in CA activity, we take advantage of the fact that active transport of DIC, the other possible cause of the light-stimulated CA activity, must saturate at high DIC concentration, whereas passive influx of  $\text{CO}_2$  does not. In *P. tricornutum*, photosynthesis is saturated at *ca.*  $500 \mu\text{M}$  DIC, and net carbon transport rates saturate with photosynthesis in all diatoms studied (6, 7). In contrast, the diffusion rate of  $\text{CO}_2$  increases linearly with DIC concentrations up to  $12,000 \mu\text{M}$  ( $[\text{CO}_2] = 80 \mu\text{M}$ ) (Fig. 1B). The relative contribution of active transport processes to  $^{18}\text{O}$  depletion must consequently decline as the DIC concentration increases. At  $\text{DIC} \gg 500 \mu\text{M}$  (say  $\text{DIC} \geq 4,000 \mu\text{M}$ ) (Discussion), any increase in the rate of  $^{18}\text{O}$  depletion in the light compared with the dark must result from an actual increase in intracellular CA activity.

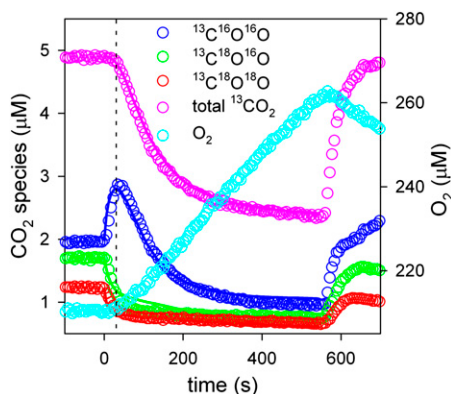


**Fig. 4.**  $^{18}\text{O}$  exchange during photosynthesis in *P. tricornutum*. A light ( $150 \mu\text{Ei/m}^2 \text{ per s}$ ) was turned on at  $t = 0$ . During the first  $\sim 45 \text{ s}$  (dashed line),  $^{18}\text{O}$  is depleted from  $^{13}\text{CO}_2$ , whereas total  $^{13}\text{CO}_2$  remains constant and  $\text{O}_2$  production is minimal. After this initiation phase, steady state photosynthesis is reached producing  $\text{O}_2$  at a constant rate and drawing down the total  $^{13}\text{CO}_2$  to support carbon fixation. Carbon fixation draws down primarily  $^{13}\text{C}^{16}\text{O}^{16}\text{O}$ , because the involvement of multiple CAs in the CCM greatly depletes  $^{18}\text{O}$  from inorganic carbon by the time that it is fixed. The lines are the fits of a single-compartment model that is described in *SI Text, One-Compartment Models, Apparent CA Activity* and diagrammed in Fig. 2.

To quantify this effect, we performed  $^{18}\text{O}$  depletion experiments in *P. tricornutum* over a range of DIC concentrations and calculated the apparent CA activity ( $k_{\text{ap}}$ ) necessary to account for the data in the dark and the light. The data are analyzed using the single-compartment model (*SI Text, One-Compartment Models, Apparent CA Activity*) as diagrammed in Fig. 2. The model is similar to the single-compartment model used to analyze passive fluxes, with the addition of terms for  $\text{HCO}_3^-$  uptake in the light and photosynthesis. The rate of  $\text{HCO}_3^-$  uptake is calculated at each time point from the experimental data as the difference between the rate of photosynthesis measured by  $\text{O}_2$  production (assuming 1  $\text{CO}_2$  fixed per  $\text{O}_2$  produced) and net  $\text{CO}_2$  uptake, itself obtained from the  $\text{CO}_2$  data corrected for the uncatalyzed rates of  $\text{CO}_2$  hydration and  $\text{HCO}_3^-$  dehydration in the external medium (*SI Text, Net Photosynthesis, CO2 Uptake, and HCO3- Uptake*) (12). The value of  $k_{\text{ap}}$ , the apparent CA activity in the cell, is obtained for each experiment by optimizing the fit of the model calculations with the experimental data.  $k_{\text{ap}}$  serves as a single parameter to quantify the extent of  $^{18}\text{O}$  depletion in the light; it accounts for both the actual enhancement of CA activity and the effects of active transport on  $^{18}\text{O}$  depletion.

As expected, there is a much larger difference between  $k_{\text{ap}}$  (light) and  $k_{\text{cf}}$  (dark) at low than at high DIC concentrations (Fig. 5). The larger enhancement of apparent CA activity in the light at low  $\text{CO}_2/\text{DIC}$  reflects the effects of active DIC transport as discussed below. The remaining enhancement at high  $\text{CO}_2/\text{DIC}$ , on average, a factor of  $2.3 \pm 0.3$  (at  $\text{DIC} \geq 4,000 \mu\text{M}$ ), is caused by an actual increase in CA activity in the light. The timescale of the  $^{18}\text{O}$  depletion is too short for synthesis of new CA enzymes. Therefore, the increase in CA activity likely reflects either a posttranslational regulation of the enzyme or a change in the chemistry of the medium. The activity of CAs increase with pH (16, 17), and pH in the chloroplast stroma rises by 0.5–1 units during photosynthesis as a result of light-driven  $\text{H}^+$  transport into the thylakoid lumen (18, 19). This is where PtCA1 is located (15), and for the purified PtCA1, an increase of 0.5–1 pH units would increase its activity by 3–10 $\times$  (Fig. S3). Acidification of the thylakoid lumen would also increase the uncatalyzed rate of  $^{18}\text{O}$  exchange in this compartment and contribute to extracellular  $^{18}\text{O}$  depletion. The small increases in cytoplasmic pH that have been measured in microalgae during photosynthesis (e.g.,  $<0.05$

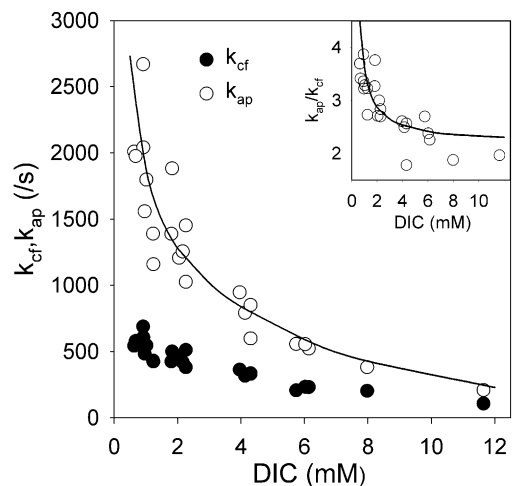


**Fig. 5.**  $^{18}\text{O}$  exchange during photosynthesis in *P. tricornutum* as a function of DIC. CA activities, indicated by the hydration rate constant, in the dark ( $k_{\text{cf}}$ ) and apparent CA activities during photosynthesis ( $k_{\text{ap}}$ ). Apparent CA activity includes true CA hydration rates and other processes that deplete  $^{18}\text{O}$  in the light such as inorganic carbon transport. The line is the  $k_{\text{ap}}$  obtained from simulations of a constant rate of  $\text{HCO}_3^-$  transport into the chloroplast ( $9 \times 10^{-17} \text{ mol/cell per s}$ ). Inset shows the ratio  $k_{\text{ap}}/k_{\text{cf}}$ , with the line derived from the simulation of  $\text{HCO}_3^-$  transport into the chloroplast.

pH units in the green alga, *Chlamydomonas reinhardtii* (20) would not significantly alter the rates of CO<sub>2</sub> hydration/HCO<sub>3</sub><sup>-</sup> dehydration whether catalyzed or not.

To account for the increased CA activity induced by light in the analyses below, we consider that this increase occurs exclusively in the chloroplast in a two-compartment model of the cells (*SI Text, CA Activity in the Chloroplast and Cytoplasm* and Table S3). Using the chloroplast dimensions measured microscopically, chloroplast CA activity must be raised on average about 16× to achieve a rise in whole-cell CA activity by a factor of 2.3. The exact value depends on the partitioning of CA between the chloroplast and cytoplasm, as discussed in *SI Text, CA Activity in the Chloroplast and Cytoplasm, Partitioning CA Activity*, but the interpretation of the data remains essentially the same provided that there is sufficient CA activity in the cytoplasm to recycle leaked CO<sub>2</sub>. The expected enhancement of PtCA1 activity because of the stromal pH rise can, thus, roughly account for the rise in whole-cell activity at high DIC concentrations when there is no significant contribution from active uptake.

**Active Transport of DIC.** Transport of DIC across the cytoplasmic or chloroplastic membrane can deplete <sup>18</sup>O by exposing <sup>18</sup>O-enriched DIC to CA. <sup>18</sup>O depletion may also be caused by so-called vectorial CA activity, the active conversion of CO<sub>2</sub> to HCO<sub>3</sub><sup>-</sup> in the cytoplasm, a process that is common in cyanobacteria (21). The details of this unidirectional hydration of CO<sub>2</sub> are not fully understood, but it results from the activity of an NAD(P)H, dehydrogenase, which may generate an alkaline pocket in the cytoplasm to drive the reaction. We investigated these various possibilities by comparing the experimental data to the results of a two-compartment box model (cytoplasm and chloroplast) that incorporates each possible process in turn. The model (*SI Text, Model for <sup>18</sup>O Exchange During Photosynthesis* and Fig. S4) is similar to the two-compartment box model used above except that passive HCO<sub>3</sub><sup>-</sup> flux across the chloroplast membrane is allowed (assuming  $P_b = 4.0 \times 10^{-6}$  cm/s, the value for the cytoplasmic membrane), chloroplast CA activity in the light is enhanced as discussed in the previous section, and the minimal chloroplast  $P_c$  value determined for the PtCA1 overexpresser is used (using a higher chloroplast permeability affects the concentrations of inorganic carbon in the model but does not alter active transport fluxes) (*Discussion*). Photosynthesis occurs in the chloroplast at the observed time-dependent rate of O<sub>2</sub> production.

Because the cytoplasmic membrane is nearly impermeable to HCO<sub>3</sub><sup>-</sup>, net HCO<sub>3</sub><sup>-</sup> transport into the cytoplasm, which is accurately measured as the difference between photosynthesis and net CO<sub>2</sub> uptake (12), is effectively equal to gross transport. There is, thus, little leeway for adjusting HCO<sub>3</sub><sup>-</sup> transport rate into the cytoplasm in the model. Unsurprisingly, if this rate is nonetheless varied, one can match the initial rise in <sup>13</sup>C<sup>16</sup>O<sup>16</sup>O, but the model then diverges from the experimental data (Fig. 6B). HCO<sub>3</sub><sup>-</sup> transport into the cytoplasm simply cannot explain the measured <sup>18</sup>O depletion.

In contrast, models that consider active CO<sub>2</sub> transport into the cytoplasm, vectorial CA activity, or DIC transport into the chloroplast provide acceptable fits to experimental data and could, in principle, explain the <sup>18</sup>O depletion caused by light (Fig. 6 C–F). However, these various processes have widely different energetic costs, and they result in widely different concentrations of CO<sub>2</sub> in the chloroplast, the *raison-d'être* of the CCM (Table 3). Vectorial CA activity and CO<sub>2</sub> transport into the cytoplasm are similar processes, because the active conversion of CO<sub>2</sub> to HCO<sub>3</sub><sup>-</sup> in the cytoplasm creates an inward CO<sub>2</sub> gradient driving diffusive CO<sub>2</sub> influx. However, neither process elevates the CO<sub>2</sub> concentration in the chloroplast much above extracellular levels (Table 3), and vectorial CA activity requires an unreasonable energetic expenditure. If vectorial CA activity was based on NAD(P)H dehydrogenase, as in cyanobacteria (21), the rate required to explain the <sup>18</sup>O depletion would consume more NAD(P)H than carbon fixation. Such a highly inefficient process is unlikely to be used. In the case of active

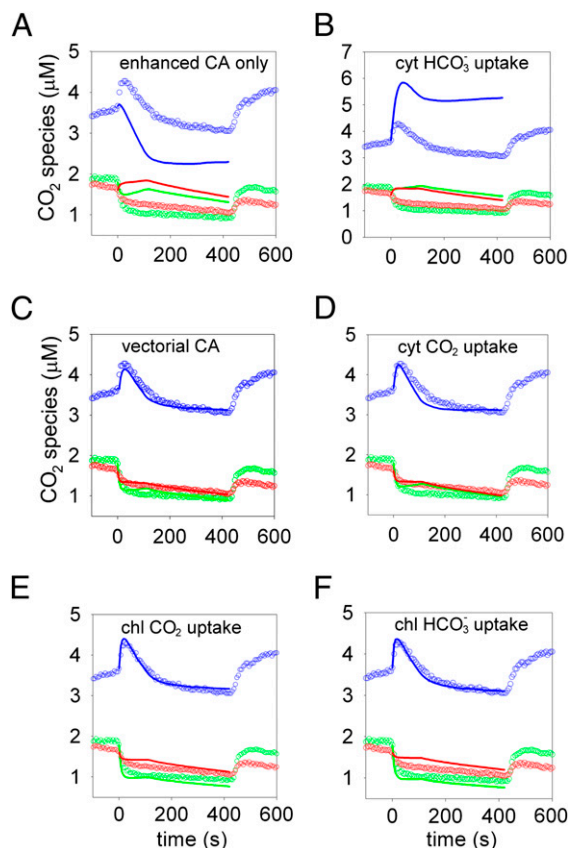


**Fig. 6.** The effect of active transport processes on <sup>18</sup>O-CO<sub>2</sub>. In all panels, the data from a sample experiment on *P. tricornutum* are shown as open circles (blue, <sup>13</sup>C<sup>16</sup>O<sup>16</sup>O; green, <sup>13</sup>C<sup>18</sup>O<sup>16</sup>O; red, <sup>13</sup>C<sup>18</sup>O<sup>18</sup>O), and model fits are solid lines. Photosynthesis was started by turning on a light at  $t = 0$ . (A) The background scenario in which CA in the chloroplast is enhanced to raise whole-cell CA activity by 2.3×. This enhanced CA activity is included in all other scenarios. (B) HCO<sub>3</sub><sup>-</sup> transport from the extracellular environment and into the cytoplasm at  $4 \times 10^{-17}$  mol/cell per s. (C) Vectorial CA activity in the cytoplasm at  $42 \times 10^{-17}$  mol/cell per s. (D) CO<sub>2</sub> transport from the extracellular environment and into the cytoplasm at  $13 \times 10^{-17}$  mol/cell per s. (E) CO<sub>2</sub> transport into the chloroplast at  $11 \times 10^{-17}$  mol/cell per s. (F) HCO<sub>3</sub><sup>-</sup> transport into the chloroplast at  $10 \times 10^{-17}$  mol/cell per s.

transport of CO<sub>2</sub> into the cytoplasm, the rates necessary to fit the <sup>18</sup>O data are roughly 4× the rate of photosynthesis. As this scenario shows, DIC accumulation using a membrane-based transporter of CO<sub>2</sub> is ineffective because of the high permeability of membranes to CO<sub>2</sub>.

Transport of inorganic carbon across the chloroplast membrane is also able to explain the <sup>18</sup>O depletion data reasonably well and does elevate the CO<sub>2</sub> concentration in the chloroplast (Fig. 6 E and F and Table 3). Because the high CA activity in the chloroplast rapidly equilibrates CO<sub>2</sub> and HCO<sub>3</sub><sup>-</sup>, transport of CO<sub>2</sub>, HCO<sub>3</sub><sup>-</sup>, or a C<sub>4</sub> compound, which is subsequently decarboxylated, into the chloroplast is effectively equivalent. In reality, the pyrenoid is likely to be the site of CO<sub>2</sub> elevation and where CA is localized (*Discussion*), making transport of HCO<sub>3</sub><sup>-</sup> or a C<sub>4</sub> compound advantageous; this is because they do not diffuse readily through biological membranes. The rate of inorganic carbon transport that best explains the excess <sup>18</sup>O depletion was determined for eight assays in which the effect of active transport on <sup>18</sup>O depletion should be detectable (DIC between 800 and 2,000 μM). The rates were quite consistent, on average, ~3× photosynthesis, and succeeded in raising the chloroplast CO<sub>2</sub> by 2–3× external levels. Transport of carbon into the chloroplast, thus, seems the only reasonable process to explain the <sup>18</sup>O depletion, because it acts as a functional CCM and does not require

**Table 3. Model evaluation**

Process	Transport rate	Residual	[CO <sub>2</sub> ] <sub>p</sub>	Fold [CO <sub>2</sub> ] rise
Vectorial CA activity	$4.2 \times 10^{-16}$	$1.6 \times 10^{-18}$	2.5	0.5
CO <sub>2</sub> transport into cytoplasm	$1.3 \times 10^{-16}$	$2.2 \times 10^{-18}$	7.0	1.4
CO <sub>2</sub> transport into chloroplast	$1.1 \times 10^{-16}$	$4.8 \times 10^{-18}$	16.1	3.2
HCO <sub>3</sub> <sup>-</sup> transport into chloroplast	$1.0 \times 10^{-16}$	$9.8 \times 10^{-18}$	13.7	2.7

Parameters used to evaluate the models were the rate of transport (mol/cell per s) required to best explain the data, the residual error in the fit, and the concentration of CO<sub>2</sub> in the chloroplast (μM). The fold rise in CO<sub>2</sub> is relative to the 5 μM extracellular CO<sub>2</sub> in this assay.

transport rates much in excess of photosynthesis; therefore, there is no unreasonable energy expenditure.

We tested if inorganic carbon transport into the chloroplast could explain the behavior of <sup>18</sup>O exchange as a function of DIC (Fig. 5) by simulating <sup>18</sup>O-CO<sub>2</sub> data using a two-compartment model with a constant rate of HCO<sub>3</sub><sup>-</sup> transport into the chloroplast ( $9 \times 10^{-17}$  mol/cell per s, the average modeled rate) and calculating from those data the apparent CA activities,  $k_{ap}$ , at each DIC concentration. The satisfactory agreement between the model simulations of  $k_{ap}$  and the observations (Fig. 5) provides a somewhat independent check on the validity of the model, because the calculations are made over a range of DIC concentrations wider than that used to calculate the chloroplastic HCO<sub>3</sub><sup>-</sup> transport rate used in the model. This agreement also shows the overall coherence of our data interpretation.

**Role of Pyrenoids.** Although pumping of inorganic carbon into the chloroplast elevates CO<sub>2</sub> above ambient levels, the concentrations are not sufficient to saturate RubisCO. The half saturation constant of *P. tricornutum*'s RubisCO for CO<sub>2</sub> is 40 μM (3), whereas the calculated average concentration of CO<sub>2</sub> in the chloroplast is 15–20 μM (Table 3 and Fig. 7A). We would expect the CO<sub>2</sub> concentration to be at least that of RubisCO's half saturation constant. A higher CO<sub>2</sub> concentration may be achieved in the pyrenoids, proteinaceous bodies within the chloroplast stroma where most of the cellular RubisCO is localized. Pyrenoids are known to be present in *P. tricornutum* and generally, in diatoms, and they are commonly thought to play a role in the CCM (3). The mechanism by which CO<sub>2</sub> is produced in the pyrenoid could either be dehydration of HCO<sub>3</sub><sup>-</sup> by a CA, such as PtCA1, or decarboxylation of a C<sub>4</sub> compound. In *P. tricornutum*, there is evidence for pyrenoid localization of other enzymes besides PtCA1, including a putative decarboxylase, which could be involved in CO<sub>2</sub> release from C<sub>4</sub> compounds. If the pyrenoid is the primary site of CO<sub>2</sub> elevation, then the CO<sub>2</sub> efflux from the chloroplast that we determined would actually originate chiefly from the pyrenoids. Taking the number and dimensions of the pyrenoids to be those observed for the β-CA clusters of the overexpresser (1.9 β-CA clusters with an average radius of 0.3 μm) (Methods), the concentration of CO<sub>2</sub> in the pyrenoids would be only 25 μM if it escaped the pyrenoid at diffusion-limited rates (SI Text, Model for <sup>18</sup>O Exchange During Photosynthesis). To raise this concentration to 60 μM, moderately above RubisCO's one-half saturation constant, the CO<sub>2</sub> transfer coefficient from the pyrenoid would need to be  $8.2 \times 10^{-10}$  cm<sup>3</sup>/s, roughly one-tenth the diffusion-limited value.

## Discussion

Our data show unequivocally that the cytoplasmic membranes of diatoms present a minimal barrier to CO<sub>2</sub> diffusion (Table 1 and Fig. 1B). Generalizing from our <sup>18</sup>O exchange data from a *P. tricornutum* strain overexpressing a chloroplast-localized CA, we infer that this is also true of the chloroplast membrane. Such high permeability to CO<sub>2</sub> has been observed in other lipid bilayers, such as red blood cell membranes (14), although studies of green algae indicate that their membranes inhibit CO<sub>2</sub> passage to some extent, with CO<sub>2</sub> permeabilities as low as  $8 \times 10^{-4}$  cm/s being reported (10, 11). Such high permeability to small un-

charged molecules presents a problem for accumulating CO<sub>2</sub>, but it is presumably also helpful in avoiding the accumulation of O<sub>2</sub>, which would lead to high concentrations of noxious reactive oxygen species in photosynthesizing cells.

We constructed an integrated description of DIC fluxes in *P. tricornutum* growing at  $\mu = 1.3$  d<sup>-1</sup> in seawater with typical DIC conditions (pH 8.15; [CO<sub>2</sub>] = 9.7 μM). This is achieved by combining (i) measurements of photosynthesis and net CO<sub>2</sub> and HCO<sub>3</sub><sup>-</sup> uptake, (ii) estimates of DIC transport into the chloroplast (based on <sup>18</sup>O exchange as a function of DIC), and (iii) calculated passive carbon fluxes (based on membrane permeabilities). As seen in Fig. 7A, there is a large diffusive exchange of CO<sub>2</sub> across the cytoplasmic membrane. Active transport of DIC into the chloroplast is about 10× larger than HCO<sub>3</sub><sup>-</sup> transport across the plasmalemma and constitutes the main driver of the CCM. Although Fig. 7A shows this DIC flux into the chloroplast as HCO<sub>3</sub><sup>-</sup> transport, we cannot distinguish the form of carbon transported, and transport of CO<sub>2</sub>, HCO<sub>3</sub><sup>-</sup>, or a C<sub>4</sub> compound, which is subsequently decarboxylated, is equivalent in our model. Approximately one-third of the DIC transported into the chloroplast is fixed by RubisCO after conversion to CO<sub>2</sub> by

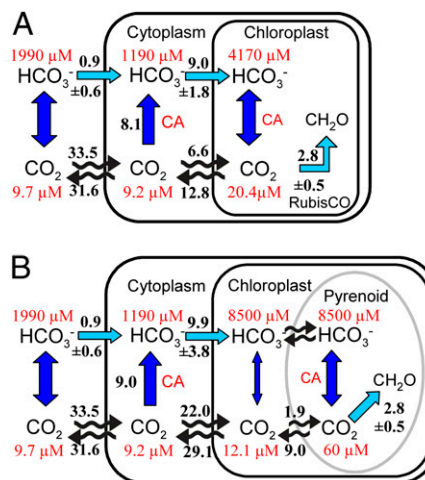


**Fig. 7.** Inorganic carbon fluxes and concentrations in *P. tricornutum*. (A) Fluxes and concentrations in an average *P. tricornutum* cell. Average rates of photosynthesis and HCO<sub>3</sub><sup>-</sup> transport were used to simulate CO<sub>2</sub> and HCO<sub>3</sub><sup>-</sup> concentrations and passive fluxes at 2,000 μM DIC ( $n \geq 8$ ). (B) Illustration of the proposed role of the pyrenoid. Here, the chloroplast is taken to have a greater permeability to CO<sub>2</sub> ( $f_c = 2.4 \times 10^{-8}$  cm<sup>3</sup>/s). The rate of HCO<sub>3</sub><sup>-</sup> uptake into the chloroplast (determined by reanalysis of the data repeating the procedure described in the text) was not significantly affected by this change. Carbon fixation and chloroplastic CA are restricted to the pyrenoid to illustrate its likely role. The pyrenoid is given a CO<sub>2</sub> transfer coefficient ( $7.9 \times 10^{-10}$  cm<sup>3</sup>/s) required to achieve 60 μM CO<sub>2</sub>, and fluxes are calculated based on this transfer coefficient. HCO<sub>3</sub><sup>-</sup> passively diffuses into the pyrenoid and is equilibrated with CO<sub>2</sub> by CA. HCO<sub>3</sub><sup>-</sup> is able to accumulate in the chloroplast, because CA is confined to the pyrenoid. Carbon fluxes are in units of  $\times 10^{-17}$  mol/cell per s.

CA. The rest diffuses as CO<sub>2</sub> into the cytoplasm, where it is recovered by CA-catalyzed hydration to HCO<sub>3</sub><sup>-</sup>.

According to our results, approximately two-thirds of net carbon uptake into *P. tricornutum* was supported by CO<sub>2</sub> diffusion, with the remaining one-third from HCO<sub>3</sub><sup>-</sup> transport. This agrees well with measurements made by others in the same organism (6). However, HCO<sub>3</sub><sup>-</sup> transport is often estimated to make up a larger fraction of net uptake in other diatoms (6, 7, 22). In all those studies, including ours, acetazolamide is present during the assays to block the activity of external CA, eCA. This should have a small effect in our strain *P. tricornutum*, which has no detectable extracellular CA activity. In other species with high eCA activity, its inhibition should often lead to a diffusion limitation of CO<sub>2</sub> transport in the boundary layer of the cell and hence, to an underestimation of the contribution of CO<sub>2</sub> to the total net carbon uptake.

Although there is no way to measure directly the gross fluxes of CO<sub>2</sub> across the cytoplasmic membrane, an independent check of our estimates of carbon fluxes based on <sup>18</sup>O loss rates is given by the <sup>13</sup>C isotopic composition of biomass (23, 24). Assuming a RubisCO fractionation factor of -29‰, the carbon fluxes shown in Fig. 7A, which are dominated by large gross CO<sub>2</sub> fluxes, produce a whole-cell δ<sup>13</sup>C fractionation of -20.4‰ relative to external CO<sub>2</sub> (SI Text, δ<sup>13</sup>C Composition of Biomass, Fig S5, and Table S4), similar to literature values for *P. tricornutum* grown at equivalent CO<sub>2</sub> concentrations (-20.5‰ to -22.0‰) (24).

The activity of a cytoplasmic CA and the maintenance of a low concentration of HCO<sub>3</sub><sup>-</sup> in the cytoplasm are key elements of the diatom CCM: they allow passive influx of CO<sub>2</sub> from the external medium and recycling of much of the CO<sub>2</sub> leaking out of the chloroplast. To support the measured rate of DIC uptake into the chloroplast, CO<sub>2</sub> must be converted to HCO<sub>3</sub><sup>-</sup> in the cytoplasm at a rate of 8.1 × 10<sup>-17</sup> mol/cell per s, but the uncatalyzed rate of CO<sub>2</sub> hydration in the cytoplasm is only ~3 × 10<sup>-20</sup> mol/cell per s. Seven putative CAs have been identified in the genome of *P. tricornutum* (25). Two β-CAs have been localized to the chloroplast (15), but one of the remaining proteins could serve to scavenge leaked CO<sub>2</sub>, either within the cytoplasm or on the endoplasmic reticulum that envelops the chloroplast. In *T. weissflogii*, there is evidence for cytoplasmic localization of a carbonic anhydrase, TWCA (26). Such localization of CA is a clear distinction between the CCM of diatoms and cyanobacteria, in which expression of a CA in the cytoplasm is highly deleterious (27).

Achieving a high concentration of CO<sub>2</sub> at the site of carbon fixation is the central function of the CCM. There seems to be little excess RubisCO carboxylation capacity in diatoms, such that near saturation of the enzyme is necessary to support observed carbon fixation rates (8). The CO<sub>2</sub> concentration at the site of fixation must, thus, be in excess of RubisCO's half saturation constant, 40 μM in *P. tricornutum* (and similar values in other diatoms) (3). However, even if we use the minimum chloroplast permeability to CO<sub>2</sub>, the average CO<sub>2</sub> concentration in the chloroplast is only 20 μM (Fig. 7A). This concentration is calculated from the diffusive CO<sub>2</sub> efflux from the chloroplast (which is constrained by the data) on the basis of the geometric characteristic of the plastid and the permeability of its envelope. If a larger chloroplast CO<sub>2</sub> permeability is used, the calculated chloroplast CO<sub>2</sub> concentration is even lower, but active transport rates are not affected (Fig. 7B). To first order, the membrane permeabilities used in the models affect only calculated passive carbon fluxes and concentrations in the cell, and they have almost no effect on derived active transport rates. This numerical result reflects the fundamental fact that the rates of <sup>18</sup>O depletion that are measured in the light require a certain carbon flux but are not directly related to intracellular carbon concentrations. It, thus, seems that the diffusion of CO<sub>2</sub> away from the site of fixation by RubisCO must be somehow more limited than in our calculation. This can result from a smaller volume in which the high CO<sub>2</sub> concentration for fixation is achieved and/or from a greater barrier to diffusion.

It is highly likely that, in *P. tricornutum*, CO<sub>2</sub> is formed in the pyrenoid where RubisCO is concentrated and carbon is fixed. The pyrenoid has a much smaller volume than the chloroplast as a whole, and because it is composed of proteins, it may be less permeable to CO<sub>2</sub> than membrane-bound compartments. Calculations show that a smaller volume is unlikely to achieve the desired results by itself, and it, thus, seems necessary that diffusion be somehow constrained (SI Text, Model for <sup>18</sup>O Exchange During Photosynthesis). To raise [CO<sub>2</sub>] to 60 μM, moderately above RubisCO's one-half saturation constant, the transfer coefficient away from the pyrenoids (which we take to be identified as PtCA1 clusters) would need to be roughly one-tenth the diffusion-limited value. It has been suggested that protein microcompartments, such as pyrenoids or carboxysomes (28), represent a greater barrier to CO<sub>2</sub> than lipid membranes. For illustration, we calculated carbon concentrations and fluxes in a model cell containing a pyrenoid but having a higher chloroplast membrane permeability to CO<sub>2</sub> (Fig. 7B). Compared with the model in Fig. 7A, the active HCO<sub>3</sub><sup>-</sup> transport rate into the chloroplast is similar, but CO<sub>2</sub> concentrations are reduced in the bulk chloroplast while being elevated to a concentration nearly saturating for RubisCO in the pyrenoid. HCO<sub>3</sub><sup>-</sup> is able to accumulate in the chloroplast, because CA activity is confined to the pyrenoid. As is commonly accepted, in this model, the pyrenoid plays a role analogous to that of the cyanobacterial carboxysome, where confinement of CA with RubisCO increases the efficiency of the CCM (3, 27).

Overall, the CCM described by the model (Fig. 7A or B) has moderate stoichiometric efficiency, requiring transport of ~3.5 molecules of inorganic carbon across the chloroplast envelope for each molecule of CO<sub>2</sub> fixed. For comparison, the marine cyanobacterium *Synechococcus* sp. WH7803 transports 6 molecules HCO<sub>3</sub><sup>-</sup> per CO<sub>2</sub> fixed, leading to CO<sub>2</sub> efflux out of the cell at 5× the rate of photosynthesis (29). The higher intracellular CO<sub>2</sub> concentration required by cyanobacterial RubisCO likely increases the CO<sub>2</sub> gradient, decreasing CCM efficiency. In *P. tricornutum*, loss of actively transported carbon only occurs across the chloroplast membrane.

Using the carbon fluxes that we measured, we can roughly estimate the amount of energy expended by *P. tricornutum* on its CCM and the potential savings from CCM down-regulation under high ambient CO<sub>2</sub>. According to our model, the only energy consumed by the CCM is caused by transport of DIC into the cytoplasm and chloroplast. In a first approximation, we consider only the carbon transport into the chloroplast, which is an order of magnitude larger than transport into the cytoplasm. If we follow Raven (2) and assume HCO<sub>3</sub><sup>-</sup> is transported into the chloroplast at a cost of 1 ATP per molecule, the need to transport ~3 HCO<sub>3</sub><sup>-</sup> molecules into the chloroplast per CO<sub>2</sub> fixed would double the ATP cost of carbon fixation. Transport of C<sub>4</sub> molecules, which require 2 ATPs per C<sub>4</sub> (30), would triple the ATP cost of carbon fixation. A substantially lower cost of transport, 0.5 ATP per HCO<sub>3</sub><sup>-</sup>, is possible if transport is driven by an H<sup>+</sup> or Na<sup>+</sup> gradient. The ~1.5–6 ATP expended on carbon transport into the chloroplast per CO<sub>2</sub> fixed adds ~75–300 kJ/mol CO<sub>2</sub> fixed, raising the energetic cost of CO<sub>2</sub> fixation by 13–51% beyond the minimum energy required to fix and reduce carbon using the Calvin cycle (hydrolysis of 3 ATP + oxidation of 2 NADPH = 590 kJ/mol) (31). A more direct constraint on the diatom CCM's energy demand should be obtainable from measurements of light use efficiency at different CO<sub>2</sub> levels (2).

Recent concern about the effects of anthropogenic CO<sub>2</sub> release on marine ecosystems has focused attention on CCMs, because their down-regulation is thought to be the primary response of phytoplankton to rising CO<sub>2</sub> (2). In our model, the major energy expended by the CCM is the transport of inorganic carbon into the chloroplast, which must compensate for the diffusive leakage of CO<sub>2</sub> away from the point of fixation. In a first approximation, the energy expended should, thus, be proportional to the [CO<sub>2</sub>] gradient between the point of fixation and the cytoplasm. Because the cytoplasmic membrane is highly permeable to CO<sub>2</sub>, its concentration is approximately the same

in the cytoplasm and external medium (Fig. 7), and the  $\text{CO}_2$  at the point of fixation (say,  $60 \mu\text{M}$ ) is presumably maintained constant by regulation of the CCM. A doubling of ambient  $[\text{CO}_2]$  to  $20 \mu\text{M}$  would then save about 20% of the CCM expenditure, decreasing the energy expended on carbon fixation between 3% and 6%, according to our estimates above. Allocation of energetic savings to carbon fixation is most likely to occur under conditions where growth is limited by energy generation—e.g., in light or iron-limited environments. In this case, the energy savings from down-regulation of the CCM on doubling of ambient  $[\text{CO}_2]$  could, thus, increase primary production by a few percent. Raising  $\text{CO}_2$  from current levels generally increases diatom photosynthesis and growth by a similar factor, if at all (7, 32, 33).

A detailed knowledge of the CCM of marine phytoplankton should provide a link between their evolution, the changing chemistry of the atmosphere, and the surface ocean over geological times. Such knowledge should also help us understand how the ongoing increase in atmospheric  $\text{CO}_2$  will affect marine primary production and the ecology of the plankton.

## Methods

**Diatom Strains and Culturing.** *T. weissflogii* [Center for the Culture of Marine Phytoplankton (CCMP) 1336], *T. pseudonana* (CCMP 1335), *T. oceanica* (CCMP 1005), and *P. tricornutum* (CCMP 632) were obtained from the CCMP and maintained in Aquil medium using natural seawater (34). For experiments, cultures were maintained at pH 8.1 in Aquil medium using a pH stat system, and cells were counted using a Coulter counter Z2. To generate the PtCA1 overexpresser, the PtCA1 sequence (15) was amplified and cloned into pENTR/D-TOPO (Invitrogen). The pENTR vector recombined with a pDEST

vector, containing diatom-specific promoters and terminators, was introduced into a native *P. tricornutum* (CCMP 632) by microparticle bombardment and transgenics selected on seawater-agar plates (35).

**MIMS.**  $^{18}\text{O}$ -labeled DIC was added to assay buffer [DIC-free artificial seawater, 20 mM Bicine, pH 8.0,  $100 \mu\text{M}$  acetazolamide (AZ)] in the MIMS chamber (36).  $^{18}\text{O}$  was monitored for  $\sim 10$  min before the addition of concentrated cells pretreated with  $100 \mu\text{M}$  AZ.  $^{18}\text{O}$  was monitored in the dark for 10–20 min and then, for  $\sim 10$  min with illumination from a tungsten lamp at  $150 \mu\text{Ei/m}^2$  per s.

**Microscopy.** The distribution of overexpressed CA linked to CFP and the size of cells and chloroplasts were determined by laser-scanning confocal microscopy. *P. tricornutum* overexpressing PtCA1 was concentrated by filtration and allowed to settle on Petri dishes with glass bottoms. The cells were imaged using a Leica SP5 microscope detecting chlorophyll fluorescence emission from 640 to 715 nm and CFP emission from 470 to 530 nm. Z stacks were obtained from several fields, and 3D objects were constructed and enumerated from the fluorescence intensities using image analysis software. The volumes of the CFP objects (PtCA1 clusters) were also determined, and an equivalent spherical radius calculated for each object.

**ACKNOWLEDGMENTS.** We thank Yan Xu for providing the purified PtCA1 enzyme and Yusuke Matsuda for providing a vector containing the PtCA1 sequence. We thank Nicolas Cassar and Philippe Tortell for providing valuable comments on the work. This study was supported by National Science Foundation Grants OCE-0722374 (to A.E.A.), OCE-0727997 (to A.E.A.), and Grant OCE-0825192 (to F.M.M.) and a grant to the Princeton Environmental Institute from BP and Ford Motor Co.

- Falkowski PG, et al. (2004) The evolution of modern eukaryotic phytoplankton. *Science* 305:354–360.
- Raven JA (1991) Physiology of inorganic C acquisition and implications for resource use efficiency by marine phytoplankton: Relation to increased  $\text{CO}_2$  and temperature. *Plant Cell Environ* 14:779–794.
- Badger MR, et al. (1998) The diversity and coevolution of Rubisco, plastids, pyrenoids, and chloroplast-based  $\text{CO}_2$ -concentrating mechanisms in algae. *Can J Bot* 76: 1052–1071.
- Reinfelder JR, Kraepiel AML, Morel FMM (2000) Unicellular  $\text{C}_4$  photosynthesis in a marine diatom. *Nature* 407:996–999.
- Roberts K, Granum E, Leegood RC, Raven JA (2007)  $\text{C}_3$  and  $\text{C}_4$  pathways of photosynthetic carbon assimilation in marine diatoms are under genetic, not environmental, control. *Plant Physiol* 145:230–235.
- Burkhardt S, Amoroso G, Riebesell U, Sültemeyer D (2001)  $\text{CO}_2$  and  $\text{HCO}_3^-$  uptake in marine diatoms acclimated to different  $\text{CO}_2$  concentrations. *Limnol Oceanogr* 46:1378–1391.
- Rost B, Riebesell U, Burkhardt S, Sültemeyer D (2003) Carbon acquisition of bloom-forming marine phytoplankton. *Limnol Oceanogr* 48:55–67.
- Glover HE, Morris I (1979) Photosynthetic carboxylating enzymes in marine phytoplankton. *Limnol Oceanogr* 24:510–519.
- Gutknecht J, Bisson MA, Tosteson FC (1977) Diffusion of carbon dioxide through lipid bilayer membranes: Effects of carbonic anhydrase, bicarbonate, and unstirred layers. *J Gen Physiol* 69:779–794.
- Tu CK, Acevedo-Duncan M, Wynns GC, Silverman DN (1986) Oxygen-18 exchange as a measure of accessibility of  $\text{CO}_2$  and  $\text{HCO}_3^-$  to carbonic anhydrase in *Chlorella vulgaris* (UTEX 263). *Plant Physiol* 80:997–1001.
- Sültemeyer D, Rinast K (1996) The  $\text{CO}_2$  permeability of the plasma membrane of *Chlamydomonas reinhardtii*: Mass-spectrometric  $^{18}\text{O}$ -exchange measurements from  $^{13}\text{C}^{18}\text{O}_2$  in suspensions of carbonic anhydrase-loaded plasma-membrane vesicles. *Planta* 200:358–368.
- Badger MR, Palmqvist K, Yu J (1994) Measurement of  $\text{CO}_2$  and  $\text{HCO}_3^-$  fluxes in cyanobacteria and microalgae during steady-state photosynthesis. *Physiol Plant* 90:529–536.
- Tu C, Wynns GC, McMurray RE, Silverman DN (1978)  $\text{CO}_2$  kinetics in red cell suspensions measured by  $^{18}\text{O}$  exchange. *J Biol Chem* 253:8178–8184.
- Silverman DN, Tu CK, Roessler N (1981) Diffusion-limited exchange of  $^{18}\text{O}$  between  $\text{CO}_2$  and water in red cell suspensions. *Respir Physiol* 44:285–298.
- Tanaka Y, Nakatsuma D, Harada H, Ishida M, Matsuda Y (2005) Localization of soluble  $\beta$ -carbonic anhydrase in the marine diatom *Phaeodactylum tricornutum*. Sorting to the chloroplast and cluster formation on the girdle lamellae. *Plant Physiol* 138:207–217.
- Silverman DN, Lindskog S (1988) The catalytic mechanism of carbonic anhydrase: Implications of a rate-limiting protolysis of water. *Acc Chem Res* 21:30–36.
- Xu Y, Feng L, Jeffrey PD, Shi Y, Morel FMM (2008) Structure and metal exchange in the cadmium carbonic anhydrase of marine diatoms. *Nature* 452:56–61.
- Heldt WH, Werdan K, Milovancev M, Geller G (1973) Alkalization of the chloroplast stroma caused by light-dependent proton flux into the thylakoid space. *Biochim Biophys Acta* 314:224–241.
- Kramer DM, Sacksteder CA, Cruz JA (1999) How acidic is the lumen? *Photosynth Res* 60:151–163.
- Braun FJ, Hegemann P (1999) Direct measurement of cytosolic calcium and pH in living *Chlamydomonas reinhardtii* cells. *Eur J Cell Biol* 78:199–208.
- Kaplan A, Reinhold L (1999)  $\text{CO}_2$  concentrating mechanisms in photosynthetic microorganisms. *Annu Rev Plant Physiol Plant Mol Biol* 50:539–570.
- Martin CL, Tortell PD (2006) Bicarbonate transport and extracellular carbonic anhydrase activity in Bering Sea phytoplankton assemblages: Results from isotope disequilibrium experiments. *Limnol Oceanogr* 51:2111–2121.
- Francois R, et al. (1993) Changes in the  $\delta^{13}\text{C}$  of surface water particulate organic matter across the subtropical convergence in the SW Indian Ocean. *Global Biogeochem Cycles* 7:627–644.
- Laws EA, Bidigare RR, Popp BN (1997) Effect of growth rate and  $\text{CO}_2$  concentration on carbon isotopic fractionation by the marine diatom *Phaeodactylum tricornutum*. *Limnol Oceanogr* 42:1552–1560.
- Kroth PG, et al. (2008) A model for carbohydrate metabolism in the diatom *Phaeodactylum tricornutum* deduced from comparative whole genome analysis. *PLoS ONE* 3:e1426.
- Morel FMM, et al. (2002) Acquisition of inorganic carbon by the marine diatom *Thalassiosira weissflogii*. *Funct Plant Biol* 29:301–308.
- Price GD, Badger MR (1989) Expression of human carbonic anhydrase in the cyanobacterium *Synechococcus* PCC7942 creates a high  $\text{CO}_2$ -requiring phenotype: Evidence for a central role for carboxysomes in the  $\text{CO}_2$  concentrating mechanism. *Plant Physiol* 91:505–513.
- Dou ZC, et al. (2008)  $\text{CO}_2$  fixation kinetics of *Halothiobacillus neapolitanus* mutant carboxysomes lacking carbonic anhydrase suggest the shell acts as a diffusional barrier for  $\text{CO}_2$ . *J Biol Chem* 283:10377–10384.
- Tchernov D, et al. (1997) Sustained net  $\text{CO}_2$  evolution during photosynthesis by marine microorganisms. *Curr Biol* 7:723–728.
- Hatch MD (1987)  $\text{C}_4$  photosynthesis—a unique blend of modified biochemistry, anatomy and ultrastructure. *Biochim Biophys Acta* 895:81–106.
- Blankenship RE (2002) *Molecular Mechanisms of Photosynthesis* (Blackwell Scientific, Oxford).
- Riebesell U, Wolf-Gladrow DA, Smetacek V (1993) Carbon dioxide limitation of marine phytoplankton growth rates. *Nature* 361:249–251.
- Tortell PD, et al. (2008)  $\text{CO}_2$  sensitivity of Southern Ocean phytoplankton. *Geophys Res Lett* 35:L04605.
- Price NM, et al. (1988) Preparation and chemistry of the artificial algal culture medium Aquil. *Biol Oceanogr* 6:443–462.
- Siaut M, et al. (2007) Molecular toolbox for studying diatom biology in *Phaeodactylum tricornutum*. *Gene* 406:23–35.
- Reinfelder JR, Milligan AJ, Morel FMM (2004) The role of the  $\text{C}_4$  pathway in carbon accumulation and fixation in a marine diatom. *Plant Physiol* 135:2106–2111.